

# Point-charge electrostatics in disordered alloys

C. Wolverton, Alex Zunger, S. Froyen, and S. -H. Wei  
 National Renewable Energy Laboratory, Golden, CO 80401  
 (May 21, 1996)

A simple analytic model of point-ion electrostatics has been previously proposed (R. Magri, S. -H. Wei, and A. Zunger, Phys. Rev. B **42**, 11388 (1990)) in which the magnitude of the net charge  $q_i$  on each atom in an ordered or random alloy depends linearly on the number  $N_i^{(1)}$  of unlike neighbors in its first coordination shell. Point charges extracted from recent large supercell (256-432 atom) local density approximation (LDA) calculations of  $\text{Cu}_{1-x}\text{Zn}_x$  random alloys now enable an assessment of the physical validity and accuracy of the simple model. We find that this model accurately describes (i) the trends in  $q_i$  vs.  $N_i^{(1)}$ , particularly for fcc alloys, (ii) the magnitudes of total electrostatic energies in random alloys, (iii) the relationships between constant-occupation-averaged charges  $\langle q_i \rangle$  and Coulomb shifts  $\langle V_i \rangle$  (i.e., the average over all sites occupied by either  $A$  or  $B$  atoms) in the random alloy, and (iv) the linear relation between the site charge  $q_i$  and the constant-charge-averaged Coulomb shift  $\bar{V}_i$  (i.e., the average over all sites with the same charge) for fcc alloys. However, for bcc alloys the *fluctuations* predicted by the model in the  $q_i$  vs  $V_i$  relation exceed those found in the LDA supercell calculations. We find that (a) the fluctuations present in the model have a vanishing contribution to the electrostatic energy. (b) Generalizing the model to include a dependence of the charge on the atoms in the first *three (two) shells* in bcc (fcc) - rather than the first shell only - removes the fluctuations, in complete agreement with the LDA data. We also demonstrate an efficient way to extract charge transfer parameters of the generalized model from LDA calculations on small unit cells.

PACS numbers: 61.66.Dk, 71.10.+x, 61.50.Lt

## I. INTRODUCTION

The structural stability of alloys and compounds is determined by the kinetic, electrostatic, and exchange-correlation contributions to the total energy. In first-principles calculations based on Hartree-Fock or on density functional theory, the electrostatic portion of the total energy is characterized in terms of the electronic charge density  $\rho(\mathbf{r})$  and the nuclear charges  $z_i$ . For systems with uniquely specified nuclear positions  $\{\mathbf{R}_i\}$  and charges  $\{z_i\}$ , the charge density is a well defined quantity as is the electrostatic (el) portion of the total energy:

$$E_{\text{el}} = \frac{1}{2} \int \int d^3\mathbf{r} d^3\mathbf{r}' \frac{\rho(\mathbf{r})\rho(\mathbf{r}')}{|\mathbf{r} - \mathbf{r}'|} - \sum_i \int d^3\mathbf{r} \frac{\rho(\mathbf{r})z_i}{|\mathbf{r} - \mathbf{R}_i|} + \frac{1}{2} \sum_i \sum_j \frac{z_i z_j}{|\mathbf{R}_i - \mathbf{R}_j|} \quad (1)$$

Indeed, in many previous calculations on ordered structures<sup>1,2,3,4,5,6,7,8</sup> and “supercell” models of random alloys,<sup>9,10</sup> there are well-defined  $\{\mathbf{R}_i; z_i\}$ , so the electrostatic energy was obtained from Eq. (1). However, in simpler approaches,<sup>11,12,13,14,15</sup> one approximates the electrostatic energy by replacing the continuous charge density  $\rho(\mathbf{r})$ , with fictitious point charges  $q_i$  at each site  $i$ . For a system with  $N$  sites, the electrostatic or Madelung (M) energy is

$$E_M = \frac{1}{2N} \sum_i \sum_{j \neq i} \frac{q_i q_j}{R_{ij}} \quad (2)$$

where  $R_{ij}$  is the distance between sites  $i$  and  $j$ . The Madelung energy may also be written

$$E_M = \frac{1}{2N} \sum_i q_i V_i \quad (3)$$

where  $V_i$  is the Coulomb shift at site  $i$  due to all charges other than  $q_i$ :

$$V_i = \sum_{j \neq i} \frac{q_j}{R_{ij}}. \quad (4)$$

The point charges are obtained by partitioning  $\rho(\mathbf{r})$  into “domains” (spheres, polyhedra, etc.) and integrating the total charge in each domain. However, because there is not a unique way to partition a three-dimensional space, the point charges are not uniquely defined.

For periodic systems (e.g., ordered structures with a *primitive* cell or random structures defined by *supercells*<sup>5,9,10,11,16,17,18</sup>) where all sites  $i$  are defined as distinct entities (not as averages) and  $q_i$  and  $\mathbf{R}_i$  are specified,  $E_M$  can be readily computed from Eq. (2) using, for example, the Ewald method. In most statistical approaches to alloys (e.g., the coherent potential approximation, or CPA)<sup>19</sup> however, one attempts a description of a random alloy without a specification of all *distinct* sites  $i$  but rather some averages over  $i$ . In such approaches one calculates the Madelung energy of the random alloy by determining the configurationally averaged correlation between charges  $\langle q_i q_j \rangle$ , and using

$$\langle E_M \rangle_R = \frac{1}{2N} \sum_i \sum_{j \neq i} \frac{\langle q_i q_j \rangle}{R_{ij}}. \quad (5)$$

Until 1990, all CPA-based models for alloy energies have assumed uncorrelated charges

$$\langle q_i q_j \rangle = \langle q_i \rangle \langle q_j \rangle \quad (6)$$

which leads to a vanishing electrostatic energy for the random alloy

$$\langle E_M \rangle_R = 0 \quad (7)$$

on account of electroneutrality. This approximation [Eq. (6)] was based on the expectation that a random (i.e. uncorrelated) distribution of *atoms* on sites would lead to an equally random distribution of *charges*, i.e., the charge on an atom in a given alloy is a property of the atom, irrespective of its environment. Eq. (7) has been assumed in many CPA-based calculations<sup>19,20,21,22,23,24</sup> involving the total energy of random alloys. Magri *et al.*<sup>11</sup> subsequently criticized this approach as being physically implausible, since the assumption of uncorrelated charges [Eq. (6)] means that an *A* atom surrounded locally by only *A* atoms will have the same charge as an *A* atom surrounded by *B* atoms; chemical intuition suggests, however, that the charge on a site will depend on the identity of atoms in its environment because charge transfer is present only between *dissimilar* sites.

Magri *et al.*<sup>11</sup> noted that in a random alloy, even though the *occupation* of site *i* is independent of the occupation of other sites by definition, the *charges* on a site do depend on the occupations of other sites. These authors therefore proposed a simple model to describe the magnitude of point charges in disordered (and ordered) alloys: The magnitude of the charge on a site is linearly proportional to the number  $N_i^{(1)}$  of unlike nearest neighbors surrounding that site. With this charge model, Magri *et al.* went on to demonstrate that even for the case of a random alloy with completely uncorrelated atomic occupations, charge correlations exist in the alloy and these correlations lead to a non-zero Madelung energy.

Subsequent to the proposal of Magri *et al.*,<sup>11</sup> the charge model has been used in many contexts:

(i) Lu *et al.*<sup>10</sup> showed that LDA calculations on ordered compounds produced charge densities which, when integrated inside muffin-tin spheres, gave point charges which reproduced the behavior of the model. They also examined<sup>5</sup> the effect of the ensuing electrostatic energy of the random alloy on the sign of the ordering energy.

(ii) Abrikosov *et al.*<sup>25</sup> and Johnson and Pinski<sup>13</sup> derived corrections to the CPA total energy which introduced charge correlations in random alloys. These corrections were shown to be consistent with the charge model of Magri *et al.* Several authors subsequently used these corrections in total-energy CPA calculations to determine lattice constants and formation energies of random metallic alloys, finding significant effects due to charge correlations: Johnson and Pinski<sup>13</sup> estimated the total energy contribution due to charge correlations to be  $-1.25$ ,  $-5.3$ , and  $-7.7$  mRy/atom for  $\text{Cu}_{0.5}\text{Zn}_{0.5}$ ,  $\text{Cu}_{0.5}\text{Au}_{0.5}$  and  $\text{Ni}_{0.5}\text{Al}_{0.5}$  alloys, respectively. (Typical values of alloy formation energies are

$\sim 10$ - $20$  mRy/atom.) Korzhavyi *et al.* found<sup>26</sup> that the energetic contribution due to charge correlations for  $\text{Al}_{0.5}\text{Li}_{0.5}$  is  $-16.0$  mRy/atom which results in a change of *sign* in the formation energy of Al-Li alloys.

(iii) Borici and Monnier<sup>12</sup> used the charge model to study the segregation behavior of a semi-infinite random Madelung lattice. For semi-infinite surface geometries, these authors found that charge correlations lead to monotonic surface segregation profiles and a segregation of the minority species to the surface. On the other hand, for thin-film geometries charge correlations lead to oscillatory surface segregation profile, and an enrichment of the majority species on the surface.

(iv) Wolverton and Zunger<sup>14</sup> determined the ground state long-range order and the high-temperature short-range order of fcc-, bcc-, and sc-based alloys due to electrostatic effects. These authors also showed<sup>1,14</sup> how the charge model could be analytically mapped onto a cluster expansion, which allowed for the efficient and accurate determination of energies of any ordered or disordered configuration without the use of Ewald methods.

(v) Ruban *et al.*<sup>15</sup> compared the energies of charge-correlated CPA calculations with ordered compound LDA calculations to determine the optimum prefactor for the electrostatic energy for Cu-Au and Ni-Pt alloys. The energetic contribution due to charge correlations was again found to be significant: For instance, for random  $\text{Cu}_{75}\text{Au}_{25}$  alloys, electrostatic contributions to the total energy were found to lower the mixing energy by a factor of  $\sim 3$ - $6$  relative to CPA calculations with a complete neglect of charge transfer effects.

The charge model ansatz of Magri *et al.* was thus far tested by comparing its charges  $\{q_i\}$  with those found in small-unit-cell ( $\leq 16$  atom) LDA calculations, and also for only one lattice type - fcc. Recently, much larger LDA supercell calculations became available<sup>16</sup> for fcc and bcc-based alloys. These calculations combine a locally self-consistent muffin-tin scheme with a massively parallel computer enabling LDA calculations on 256- and 432-atom supercells for random Cu-Zn alloys.<sup>17,18</sup> Faulkner *et al.*<sup>17,18</sup> have used the charge density from these large LDA supercells to examine the behavior of point charges  $\{q_i\}$  in random Cu-Zn alloys, finding interesting relations between charges and certain potentials. Here we determine to what extent the simple charge model is able to describe the electrostatic properties of complicated large scale (256-432 atom) LDA based calculations. We find that the model works very well for fcc lattices, but that in bcc lattices, where the first few coordination shells are near to one another, the charge on a site is correlated with the occupations on a *few* neighboring shells, not just one. The effects of such corrections to the total electrostatic energy  $\langle E_M \rangle_R$  are small, however.

## II. THE SIMPLE CHARGE MODEL

Consider an  $A_{1-x}B_x$  alloy with  $N$  sites and a nearest neighbor coordination number  $Z$ . The model of Magri *et*

*al.*<sup>11</sup> is based on the assumption that the excess charge on a site depends only on the identity of its *first* neighbors. If an *A* atom on a central site is surrounded purely by *Z* atoms of type *A*, the charge is taken to be zero. If it is surrounded by *Z* atoms of type *B*, the charge is maximal,  $2Z\lambda$ . For intermediate occupations of the first coordination shell, we assume a linear interpolation between these two limits. Formally, we then write this charge as:

$$q_i = \lambda \sum_{k=1}^Z [\hat{S}_i - \hat{S}_{i+k}], \quad (8)$$

where the pseudospin  $\hat{S}_i$  is -1 (+1) if an *A*(*B*) atom is located at site *i*. (The set of variables  $\hat{S}_i$  for all sites *i* defines the configuration  $\sigma$ .)  $\hat{S}_{i+k}$  indicates the occupation of the *Z* lattice sites which are nearest neighbors to *i*, and hence the summation in Eq. (8) indicates the number of unlike nearest neighbors surrounding the site *i*.  $\lambda$  is a constant which indicates the magnitude of the charge transfer and is an undetermined parameter of the model. Thus, the charge model will give trends in the behavior of physical properties, but will not give numerical values of properties without some input value of  $\lambda$ .

Several questions may be asked concerning the parameter  $\lambda$ : 1) Should  $\lambda$  be explicitly composition-dependent? 2) Should  $\lambda$  be explicitly volume-dependent? Since the equilibrium volume is a function of composition in size-mismatched alloys, an explicit volume dependence of  $\lambda$  would lead to an implicit composition-dependence. It is important to physically distinguish between these two dependences. 3) Should the values of  $\lambda$  be extracted from large unit cell or small unit-cell alloys i.e., does  $\lambda$  contain mostly short-range or long-range information? Values of  $\lambda$  have been estimated by LDA calculations,<sup>10,13,18</sup> ranging from small unit cell ordered compounds ( $\sim 8$ -16 atoms), up to large LDA simulations of random alloys ( $\sim 200$ -400 atoms). For computational simplicity, one should know whether it is equally valid to extract values of  $\lambda$  from ordered or random alloys, and whether one can even use smaller cells ( $\sim 2$ -4 atoms) than have been currently used.

We next examine the physical consequences of charges which obey Eq. (8). We then compare these consequences with results of LDA supercell calculations in order to assess the physical validity of the model. With regard to the questions raised above, we demonstrate that the simple charge model represents well the charge transfer of *different* unrelaxed configurations at a *common* volume. If more than one volume is considered (e.g., for a lattice-mismatched alloy at more than one composition), the parameter of the model  $\lambda$  would presumably need to be explicitly volume-dependent (implicitly composition-dependent). Also, we find that values of  $\lambda$  extracted from 2-4 atom LDA calculations agree favorably with those extracted from much larger 200-400 atom LDA calculations, thereby resulting in a drastic computational simplification.

### III. PHYSICAL CONSEQUENCES OF THE CHARGE MODEL

#### A. Average Charges

The average charge *on all sites*,  $\langle q \rangle$  is defined as:

$$\langle q \rangle = \frac{1}{N} \sum_i q_i \quad (9)$$

Combining this with Eq. (8) gives  $\langle q \rangle = 0$ , as guaranteed by global charge neutrality. However, what is more interesting is the constant-occupation-average  $\langle q \rangle_A$  (or  $\langle q \rangle_B$ ), i.e., the average charge of all sites occupied by *A* (*B*) atoms. This constant-occupation-average is a function of the configuration  $\sigma$  and composition *x*, and we can analytically derive this quantity for any arbitrary configuration. The definition of  $\langle q \rangle_A$  is

$$\langle q \rangle_A = \frac{1}{N_A} \sum_i q_i \Gamma_i^A, \quad (10)$$

where  $N_A$  is the number of *A* atoms in  $\sigma$  and  $\Gamma_i^A$  is the Flinn operator such that  $\Gamma_i^A = 1$  if site *i* is occupied by an *A* atom, and  $\Gamma_i^A = 0$  otherwise. The Flinn operator is given by  $\Gamma_i^A = (1 - \hat{S}_i)/2$ . Thus,

$$\begin{aligned} \langle q \rangle_A &= \frac{\lambda}{2N_A} \sum_i \sum_k (\hat{S}_i - \hat{S}_{i+k} - \hat{S}_i^2 + \hat{S}_i \hat{S}_{i+k}) \\ &= -\frac{Z\lambda}{2(1-x)} (1 - \bar{\Pi}) \end{aligned} \quad (11)$$

where  $\bar{\Pi}$  is the nearest neighbor (NN) pair correlation function, i.e., the lattice average of  $\Pi_{i,j} = \hat{S}_i \hat{S}_j$  for *i* and *j* NN. A similar analysis gives

$$\langle q \rangle_B = \frac{Z\lambda}{2x} (1 - \bar{\Pi}) \quad (12)$$

In addition, the difference  $\Delta$  in constant-occupation-averaged charges is given by

$$\Delta = \langle q \rangle_B - \langle q \rangle_A = 2Z\lambda \frac{1 - \bar{\Pi}}{1 - \langle S \rangle^2} \quad (13)$$

where  $\langle S \rangle = 2x - 1$ . Equations (11), (12), and (13) are quite general and apply to any configuration (ordered, random, or partially ordered). These expressions may be evaluated in various classes of configurations which are interesting:

*Random Alloys:* We define a random alloy as one in which the *occupation variables*  $\hat{S}_i$  are uncorrelated, i.e.  $\bar{\Pi}_{i,j} = \langle S_i \rangle \langle S_j \rangle \equiv (2x - 1)^2$ . As we will see below, this does not imply that the *charges*  $q_i$  are uncorrelated. In a random alloy, we have

$$\langle q \rangle_A = -2Z\lambda x ; \quad \langle q \rangle_B = 2Z\lambda(1-x) ; \quad \Delta = 2Z\lambda \quad (14)$$

Interestingly,  $\Delta$  for random alloys is independent of alloy composition *x*.

*Short-range Ordered Alloys:* Short-range order (SRO) measures the extent to which there are atom-atom correlations in a disordered alloy. The relation between the nearest neighbor Warren-Cowley SRO parameter ( $\alpha$ ) and  $\bar{\Pi}$  is

$$\alpha = \frac{\bar{\Pi} - \langle S \rangle^2}{1 - \langle S \rangle^2}. \quad (15)$$

This expression combined with Eqs. (11) and (12) and (13) gives the constant-occupation-averaged charges for alloys possessing some degree of SRO:

$$\begin{aligned} \langle q \rangle_A &= -2Z\lambda x(1 - \alpha) \quad ; \quad \langle q \rangle_B = 2Z\lambda(1 - x)(1 - \alpha) \quad ; \\ \Delta &= 2Z\lambda(1 - \alpha) \end{aligned} \quad (16)$$

So, the difference in charges  $\Delta$  should increase in an ordering type alloy ( $\alpha < 0$ ) relative to the random values, but should decrease in a clustering type alloy ( $\alpha > 0$ ).

*Long-range Ordered Alloys:* Long-range order (LRO) gives an indication for the relative population of  $A$  or  $B$  atoms on a given sublattice. The extent of LRO in an alloy may be described by (one or more) LRO parameters  $\eta$ . For example, for an alloy at  $x=1/2$  with a single LRO parameter  $0 \leq \eta \leq 1$  (and no correlations between atoms on the same sublattice),  $\bar{\Pi}(\eta) = \eta^2 \bar{\Pi}(1)$ , so for any state of LRO at  $x=1/2$ :

$$\begin{aligned} \langle q \rangle_A(\eta) &= -Z\lambda[1 - \eta^2 \bar{\Pi}(1)] \quad ; \\ \langle q \rangle_B(\eta) &= Z\lambda[1 - \eta^2 \bar{\Pi}(1)] \quad ; \\ \Delta(\eta) &= 2Z\lambda[1 - \eta^2 \bar{\Pi}(1)] \end{aligned} \quad (17)$$

For example, in CsCl ( $B2$ ) type ordering  $\bar{\Pi}(1) = -1$ , thus as the degree of LRO increases,  $\Delta$  increases due to the increased number of unlike nearest neighbors.

### B. Constant-Occupation-Averaged Coulomb Shifts, $\langle V \rangle_A$ and $\langle V \rangle_B$

The Coulomb shift  $V_i$  [Eq. (4)] averaged over all sites  $\langle V \rangle$  is zero (just as  $\langle q \rangle$  is zero) due to global neutrality. A more interesting quantity is the constant-occupation-average of the Coulomb shifts on all sites occupied by  $A$ -atoms in a random alloy:

$$\langle V \rangle_A = \frac{1}{N_A} \sum_i \langle V_i \Gamma_i^A \rangle. \quad (18)$$

where the latter brackets denote a configurational average. This expression can be evaluated to give:

$$\begin{aligned} \langle V \rangle_A &= \frac{\lambda}{2(1-x)} \left\langle \sum_{j \neq i} \sum_k \frac{1}{R_{ij}} (\hat{S}_j - \hat{S}_{j+k})(1 - \hat{S}_i) \right\rangle \\ &= \frac{\lambda}{2(1-x)} \sum_{j \neq i} \sum_k \frac{1}{R_{ij}} [1 - (2x-1)^2] \delta_{i,j+k} \\ &= \frac{2xZ\lambda}{R_1} \end{aligned} \quad (19)$$

where  $R_1$  is the nearest-neighbor distance and in the second equality of Eq. (19), we have used the orthonormal properties of the products of  $\hat{S}_i$ .<sup>27</sup> Similarly for  $B$ -atoms,

$$\langle V \rangle_B = -\frac{2(1-x)Z\lambda}{R_1} \quad (20)$$

### C. Relation between Constant-Occupation-Averaged Charge and Coulomb Shift

From Eqs. (14) and (19), we have the following relation between constant-occupation-averaged charge and Coulomb shift, as predicted by the charge model:

$$\langle V \rangle_{A,B} = \frac{-\langle q \rangle_{A,B}}{R_1} \quad (21)$$

### D. Charge-Charge Correlation Functions

The charge-charge correlation function between sites  $i$  and  $j$  is given by:

$$\begin{aligned} \langle q_i q_j \rangle &= \frac{1}{N} \sum_{m=1}^N q_{i+m} q_{j+m} \\ &= \lambda^2 [Z^2 \bar{\Pi}_{i,j} - Z \left( \sum_{k=1}^Z \bar{\Pi}_{i+k,j} + \sum_{k'=1}^Z \bar{\Pi}_{i,j+k'} \right) \\ &\quad + \sum_{k=1}^Z \sum_{k'=1}^Z \bar{\Pi}_{i+k,j+k'}] \end{aligned} \quad (22)$$

The sums over  $k$  ( $k'$ ) are over the nearest neighbors of site  $i$  ( $j$ ). Eq. (22) is generally valid for any configuration and any composition. For random alloys (i.e., alloys with uncorrelated site occupations), the charge correlations for the  $m$ th shell  $\langle q_0 q_m \rangle$  have been previously derived<sup>5</sup> and are given by:

$$\begin{aligned} \langle q_0 q_0 \rangle &= 4x(1-x)\lambda^2(Z_1^2 + Z_1) \\ \langle q_0 q_1 \rangle &= 4x(1-x)\lambda^2(-2Z_1 + K_1) \\ \langle q_0 q_m \rangle &= 4x(1-x)\lambda^2(K_m) \quad ; \quad m > 1 \end{aligned} \quad (23)$$

In these expressions,  $Z_m$  is the coordination of the  $m$ th shell (i.e.,  $Z_1 \equiv Z$ ), and  $K_m$  is the number of nearest-neighbor atoms shared by sites  $i$  and  $i+m$ . As found by Magri *et al.*<sup>11</sup>, Eqs. (23) demonstrate that even when the *occupations* of sites are uncorrelated, the *charges* on these sites, obeying Eq. (8), are correlated.

### E. Electrostatic Energies of Random Alloys

Using the charge-charge correlations in Eq. (23), one can obtain the electrostatic energies of random alloys which are a consequence of the charge model. These

energies of random alloys have been derived previously for fcc, bcc, and sc-based alloys.<sup>11,14</sup> The energies of fcc and bcc-based random alloys are given by

$$\begin{aligned}\langle E_M \rangle_R^{\text{fcc}}/E_0 &= -4x(1-x)0.7395181\dots \\ \langle E_M \rangle_R^{\text{bcc}}/E_0 &= -4x(1-x)0.3457752\dots\end{aligned}\quad (24)$$

where  $E_0 = (16\lambda)^2/2R_1$ .

### F. The $q - V$ Relation between Charges and Coulomb Shifts

For a completely random alloy, we may analytically derive (Appendix A) a relation between the charges  $q_i$  and Coulomb shifts  $V_i$  from the charge model: In the model of Eq. (8), the magnitude of the charge on a site  $i$  surrounded by  $N_i^{(1)}$  unlike neighbors in the first shell does not depend on the spatial configuration of the  $N_i^{(1)}$  and is  $|q_i[N_i^{(1)}]| = 2\lambda N_i^{(1)}$ . The Coulomb shift  $V_i[N_i^{(1)}]$  on a site surrounded by  $N_i^{(1)}$  unlike nearest neighbors on the other hand, does depend in the model of Eq. (8) on the spatial configuration of the  $N_i^{(1)}$  unlike atoms around  $i$  and also depends on more distant neighbors. If we *average* over all sites having  $N_i^{(1)}$  unlike neighbors, we find analytically (Appendix A) the linear relation between charge  $q_i[N_i^{(1)}]$  and the constant-charge-averaged Coulomb shift  $\bar{V}_i[N_i^{(1)}]$ : (i.e., an average over all sites with the same charge, and hence with the same  $N_i^{(1)}$ ),

$$q_i[N_i^{(1)}] \propto \bar{V}_i[N_i^{(1)}], \quad (25)$$

where  $\gamma$  (in  $\text{Ry}^{-1}$ ) is the slope of this linear relation:

$$\begin{aligned}\gamma_{\text{fcc}}(x=1/2) &= 0.132R_1 \\ \gamma_{\text{bcc}}(x=1/2) &= 0.163R_1\end{aligned}\quad (26)$$

Note that  $\bar{V}_i$  is a constant-charge-average (still leaving the  $N_i^{(1)}$  dependence), in contrast to the constant-occupation-averaged  $\langle V \rangle_A$ . To evaluate the *fluctuations* in  $V_i(N_i^{(1)})$  about  $\bar{V}_i$ , we perform large-unit-cell simulations for a single, randomly selected configuration. Equal numbers of atomic types  $A$  and  $B$  ( $x=1/2$ ) are distributed at random over the 256 fcc sites and 432 bcc sites of the simulation cell. Point charges  $\{q_i\}$  are then assigned by the model of Eq. (8). Using the Ewald method, we then calculate the Coulomb shifts  $V_i$  [Eq. (4)] for each site in the cell. This gives a  $q_i$  vs.  $V_i$  relation for the charge model.

## IV. COMPARISON: SIMPLE MODEL VS. LDA SIMULATIONS

Recently,<sup>17,18</sup> large scale LDA supercell calculations (256- and 432-atom) have been performed for Cu-Zn alloys with Cu and Zn atoms placed randomly on the fcc or

bcc lattice sites of the supercell. These calculations utilize a multiple scattering framework, and are locally self-consistent: The charge density associated with each atom is constructed by considering only the electronic multiple scattering processes in a finite spatial region (several neighboring shells) centered at that atom. These LDA calculations also use the muffin-tin approximation: The charge within the Wigner-Seitz cell surrounding each site  $i$  (volume  $\Omega_i$ ) is made of a spherically symmetric portion  $\rho^i(\mathbf{r}) = \rho_{\text{MT}}^i(r)$  inside each muffin-tin sphere ( $r < R_{\text{MT}}^i$ ) and is equal to a constant  $\rho_0$  in the interstitial region between spheres. Point charges are then extracted from the muffin-tin charge density by performing the following integral:

$$q_i = 4\pi \int_0^{R_{\text{MT}}^i} \rho_{\text{MT}}^i(r)r^2 dr + \rho_0[\Omega_i - \frac{4\pi}{3}(R_{\text{MT}}^i)^3] - z_i \quad (27)$$

The calculations are carried out for unrelaxed geometries, thus each of the 256 or 432 atoms has an equivalent Wigner-Seitz cell. Cu and Zn have a very small electronegativity difference, so Madelung energy is quite small in Cu-Zn alloys, and could be more susceptible to any errors in the calculation. Cu-Zn is therefore a critical test of any charge model, as the electrostatic effects in this system are quite subtle. An alloy system with more robust charge transfer (larger electronegativity difference) could therefore be of interest in comparing magnitudes of electrostatic energies, charges, and other properties.

Differences of  $\sim 2\%$  are cited<sup>17</sup> between LDA calculations using bcc cells of 256 and 432 sites, and hence indicate a typical error due to using a finite-sized supercell. An additional consideration is that one, single configuration is considered rather than a configurational average. Thus, in comparing properties of the charge model with those of LDA supercell calculations, only disparities of more than a few percent should be considered meaningful.

### A. Dependence of Charges on the Nearest-neighbor Environment

The prediction of the model of Eq. (8) for the dependence of charge on the number of unlike-nearest neighbors is clear: It is a linear relation. The charges predicted by this simple model (open circles) are compared with those obtained in extensive LDA supercell calculations (crosses)<sup>18</sup> in Fig. 1. A least-squares fit to the LDA supercell data gives values of the parameter  $\lambda$ :

$$\lambda^{\text{fcc}} = 0.00819, \quad \lambda^{\text{bcc}} = 0.01176. \quad (28)$$

The LDA calculations demonstrate that (i) the linear prediction of the model is accurate for fcc alloys, but (ii) for bcc alloys, as recognized by Faulkner *et al.*,<sup>17,18</sup> there are fluctuations about the straight line. Recall that in an fcc structure the distances from the origin to the  $n^{\text{th}}$  shell

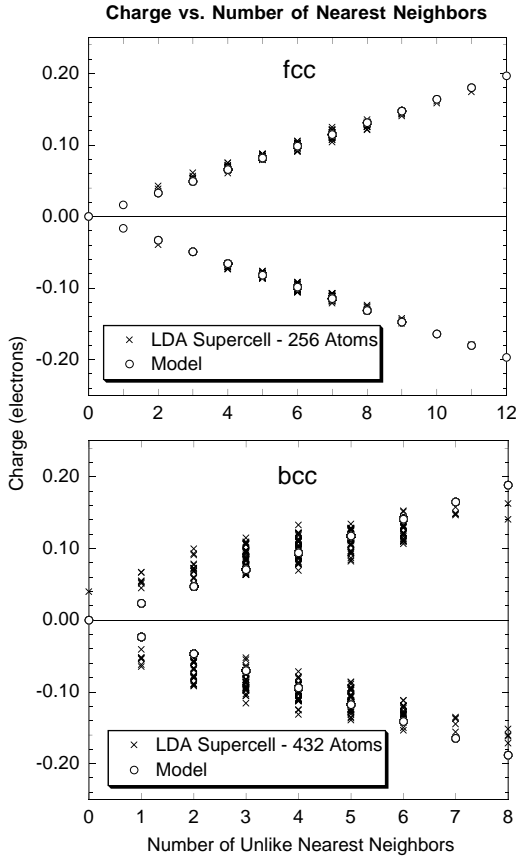


FIG. 1. Charge versus number of unlike nearest neighbors. Shown are the predictions of the charge model of Eq. (8) and the results of LDA supercell calculations of Ref. 18. Values of  $\lambda$  [Eq. (28)] were obtained by a least-squares fit to the LDA supercell data.

are  $R_1$ ,  $1.414R_1$ , and  $1.732R_1$  for  $n=1,2,3$ , while for bcc these distances are  $R_1$ ,  $1.155R_1$ , and  $1.633R_1$ . Thus, the bcc structure shows a weaker distinction between first and second neighbors. We consider below (Section V) possible generalizations of the charge model for bcc alloys which account for these fluctuations by extending the linear relation (8) to more than one coordination shell.

## B. Relation between Constant-Occupation-Averaged Charge and Coulomb Shift

Both the charge model of Eq. (8) and the LDA supercell calculations result in a relationship between the constant-occupation-averaged charges  $\langle q \rangle_A$  and  $\langle q \rangle_B$  [Eq. (14)] and the constant-occupation-averaged Coulomb shifts  $\langle V \rangle_A$  and  $\langle V \rangle_B$  [Eq. (19)] of the form:

$$\langle V \rangle_{A,B} = \frac{-\langle q \rangle_{A,B}}{R_{\text{eff}}} \quad (29)$$

According to Eq. (21), the charge model of Eq. (8) gives  $R_{\text{eff}} = R_1$  (where  $R_1$  is the nearest neighbor distance). Values of  $R_{\text{eff}}/R_1$  for the charge model and for the LDA

supercell calculations are compared in Table I. The simple charge model of Eq. (8) reproduces  $R_{\text{eff}}/R_1$  of the LDA supercell calculations (0.97 and 1.02 for fcc and bcc, respectively) to within a few percent.

In Eq. (14), it is shown that the simple charge model predicts that the difference  $\Delta$  in constant-occupation-averaged charges is independent of composition. The LDA supercell results (Fig. 3 of Ref. 17) also show that  $\Delta$  depends very little on composition, in agreement with the model prediction.

The difference between constant-occupation-averaged charges  $\Delta(\eta)$  for the charge model was also derived as a function of LRO parameter in Eq. (17). The charge model prediction is that  $\Delta(\eta)$  should increase for the LRO  $B2$  alloy relative to the random alloy by a factor  $\Delta^{B2}(1)/\Delta(0) = 2$ . The LDA calculations<sup>17</sup> show that the introduction of LRO does increase  $\Delta$  from a value of 0.20066 for the random alloy to 0.25178 for the  $B2$  ordered alloy, giving  $\Delta^{B2}(1)/\Delta(0) = 1.25$ , somewhat smaller than but qualitatively consistent with the prediction of the charge model. In considering the disparity between the magnitude of  $\Delta^{B2}(1)/\Delta(0)$  of the simple charge model and that of LDA, one should remember that in the latter, point charges are defined by a non-unique partitioning of space.

The influence of SRO on  $\Delta$  was derived for the charge model in Eq. (16) where it was shown that ordering type SRO (as found in Cu-Zn alloys) should increase  $\Delta$  relative to the random alloy. The introduction of SRO in the LDA supercell calculations<sup>17</sup> increases  $\Delta$  from 0.20066 for a random simulation to 0.20554 in a simulation with some degree of SRO. This increase is again consistent with the predictions of the charge model.

## C. The $q - V$ Relation between Charges and Coulomb Shifts

The large supercell LDA calculations find a linear relationship between the charges  $q_i$  on individual sites and the Coulomb shifts  $V_i$  on those sites. The simple charge model of Eq. (8) predicts [Eq. 25] a linear behavior between charge and constant-charge-averaged Coulomb shift in agreement with the LDA supercell calculations. The slope  $\gamma$  of this linear relation is compared with the slopes from the LDA supercell calculations in Table I. (Note that both charge and Coulomb shift are proportional to the parameter  $\lambda$  of the model, and thus, the slope  $\gamma$  is independent of  $\lambda$ .) The relative slope  $\gamma/R_1$  of the model (-0.132) is within a few percent of the LDA supercell results for fcc alloys ( $-0.125 \pm 0.002$ ), while for bcc alloys, the slope of the model (-0.163) is too large in magnitude relative to the LDA result ( $-0.115 \pm 0.001$ ).

The relationship between  $q_i$  and the distinct Coulomb shift  $V_i$  (not the constant-charge-averaged  $\bar{V}_i$ ) as obtained in the simple model of Eq. (8) is shown in Fig. 2, where it is contrasted with the results of the LDA calculations of Ref. 18. The fluctuations in Coulomb shift about the average linear behavior of  $q_i$  and  $V_i$  are quite

TABLE I. Comparison of physical properties of random alloys which are a consequence of (a) the charge model of Eq. (8), (b) the generalized charge model of Eq. (34), and (c) those obtained from LDA supercell simulations of Refs. 17, 18. In cases (a) and (b), we assign charges to sites according to a given model [Eq. (8) or (34)] and then calculate the Coulomb shift  $V_i$  [Eq. (4)] by applying the Ewald method to the assigned charges.

	$R_{\text{eff}}/R_1$	$\gamma/R_1$ [Ry $^{-1}$ *a.u. $^{-1}$ ]	$\langle E_M \rangle_R$ [mRy/atom]
fcc ( $x=1/2$ )			
Model - Analytic	1.00	-0.132	-2.60
Model - 256 atoms	1.06	-0.130	-2.52
Model - 16 atom SQS	0.99	-0.134	-2.60
LDA supercell - 256 atoms	0.97	-0.123,-0.127	-2.61
Gener. model - 256 atoms	1.02	-0.120	-2.55
Gener. model - 16 atom SQS	1.03	-0.118	-2.52
bcc ( $x=1/2$ )			
Model - Analytic	1.00	-0.163	-2.57
Model - 432 atoms	0.98	-0.155	-2.64
LDA supercell - 432 atoms	1.02	-0.114,-0.116	-2.67
Gener. Model - 432 atoms	1.19	-0.119	-2.34

small in the fcc random alloy, but are substantial in the bcc alloy. We have next determined the effect of these fluctuations on the electrostatic energy  $\langle E_M \rangle_R$  of the random alloy: If the linear relation Eq. (25) between charge and Coulomb shift (neglecting fluctuations) is used in Eq. (3) to compute the random alloy energy, we recover precisely the same energy *including fluctuations* derived in Eq. (24). Thus, although the fluctuations in  $V_i$  are graphically impressive (Fig. 2), *the energetic consequence of these fluctuations is strictly zero*, simply indicating that the fluctuations in Coulomb shift are symmetrical about the average linear behavior.

#### D. Charge-Charge Correlations Functions

The simple charge model predicts specific values for the charge-charge correlations of random alloys given in Eq. (23). The quantitative results of the LDA supercell for these correlations are a bit unclear: In Ref.<sup>18</sup>, the authors note that for 256-atom LDA supercell calculations, the nearest-neighbor correlations are sizeable, but they also note that the values beyond the nearest-neighbor shell are smaller than the predictions of the model, although these values are not too well known due to the relatively small size of the simulation cell. When larger LDA supercell simulations become available, a comparison of charge-charge correlations from LDA supercell with the predictions of Eq. (23) (and those of the generalized charge model described below) would be of interest. The analytic values of the charge-charge correlation functions of Eq. (23) are plotted in Fig. 3. We have also compared these analytic values with those obtained from our large-unit-cell simulations of the charge model (not shown). Although the correlations for the nearest neighbor shell are robust with respect to unit cell size, the correlations

for the more distant 3rd, 4th, and 5th shells are extremely sensitive to the size of the simulation cell: For a single fcc 256-atom simulation, one can even find 3rd and 4th neighbor correlations which have opposite sign relative to the exact analytic values. Even for very large (16384-atom) fcc simulations configurationally averaged over 20 configurations, the 3rd and 4th neighbor correlations may differ from the analytic values by  $\sim 10\%$ . Thus, in order to compare the LDA charge-charge correlations for random alloys with the analytic results of the simple charge model, the size of the LDA supercell calculations would have to be significantly increased.

#### E. Coulomb Energy of Random Alloys

The Madelung energy of the simple charge model for a random alloy is given in Eq. (24) in terms of the parameter  $\lambda$  and the nearest-neighbor distance  $R_1$ . If we use the numerical values for  $\lambda$  given in Eq. (28) and the nearest neighbor distances used in the LDA supercell calculations for Cu-Zn alloys,

$$R_1^{\text{fcc}} = 4.879\text{a.u.}; \quad R_1^{\text{bcc}} = 4.763\text{a.u.}, \quad (30)$$

we obtain the electrostatic energies of the simple charge model for Cu-Zn:

$$\begin{aligned} \langle E_M \rangle_R(\text{fcc}; x = 0.5) &= -2.60 \text{ mRy/atom}, \\ \langle E_M \rangle_R(\text{fcc}; x = 0.7) &= -2.18 \text{ mRy/atom}, \\ \langle E_M \rangle_R(\text{bcc}; x = 0.5) &= -2.57 \text{ mRy/atom}. \end{aligned} \quad (31)$$

These values are compared with the Cu-Zn LDA supercell values<sup>18</sup> in Table I:

$$\begin{aligned} \langle E_M \rangle_R(\text{fcc}; x = 0.5) &= -2.61 \text{ mRy/atom}, \\ \langle E_M \rangle_R(\text{fcc}; x = 0.7) &= -2.20 \text{ mRy/atom}, \\ \langle E_M \rangle_R(\text{bcc}; x = 0.5) &= -2.67 \text{ mRy/atom}. \end{aligned} \quad (32)$$

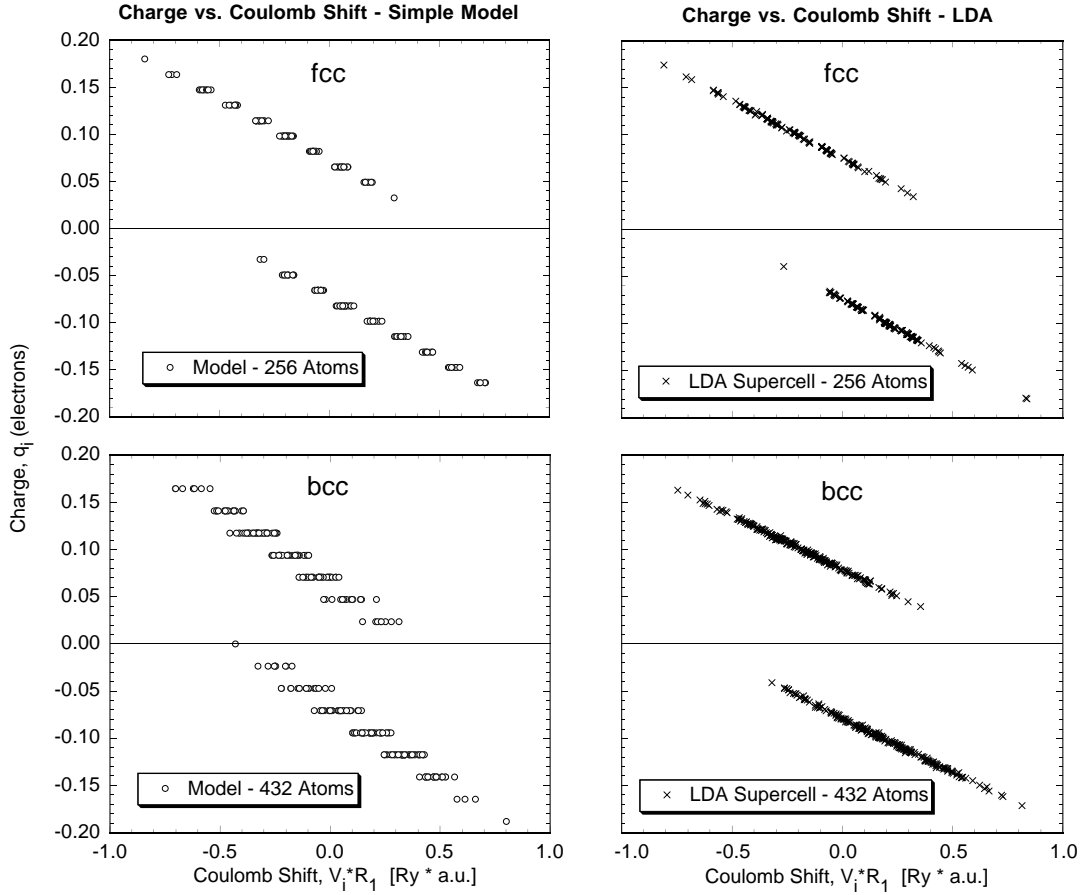


FIG. 2. Charges versus Coulomb Shifts as predicted by the charge model of Eq. (8) using the values of  $\lambda$  and  $R_1$  given in Eqs. (28) and (30). Also shown are the results of LDA supercell calculations of Ref. 18.

For all cases, the prediction of the simple model is extremely accurate: the model energies fall within 0.1 mRy of the LDA supercell calculations. Although the model of Eq. (8) was shown to have significant fluctuations in the  $q - V$  relations (Fig. 2), *these fluctuations have a vanishing contribution to the Coulomb energy*, and thus the model produces accurate energetics.

#### F. Approximating Large Random Supercells by Small-Cell “Special Quasi-Random” Structures

Our foregoing discussions were based on (either LDA or Ewald) simulations of rather large supercells (e.g., 256-432 atom). We next examine the extent to which *specialy selected* small cells can mimic larger, non-specialy selected cells. Special quasi-random structures (SQS)<sup>9</sup> are small unit-cell structures which are constructed in such a way so that structural (not charge-charge) correlation functions  $\overline{\Pi}_{\text{SQS}}$  match as closely as possible those of the random alloy ( $\overline{\Pi}_{\text{SQS}} \sim \overline{\Pi}_{\text{Random}}$ ) for several neighboring shells. In this way the SQS is a small-unit-cell ordered structure which mimics the random alloy. It is interesting to see how the charge model calculation of a small-unit-cell SQS compares with the large scale 256-

atom simulations described above.

We have performed an Ewald calculation for a 16-atom, fcc-based SQS structure (denoted SQS-16) with point charges taken from the charge model of Eq. (8). Structural information for SQS-16 is given in Appendix B. The resulting  $R_{\text{eff}}/R_1$ ,  $\gamma/R_1$ ,  $\langle E_M \rangle_R$ , and the  $q - V$  relation for the SQS-16 are collected in Table I, where they are compared with analogous calculations using a (randomly selected) 256-atom cell. We see that the 16-atom SQS calculation matches the 256-atom simulation for all properties to within a few percent. Also, the electrostatic energy of the SQS-16  $\langle E_M \rangle_{\text{SQS}}/E_0 = -0.740$  compares much more favorably with the exact value of  $-0.7395$  than does the energy of the 256-atom simulation  $\langle E_M \rangle_R^{256\text{-atom}}/E_0 = -0.716$ . Thus, for the case of electrostatic energies, the 16-atom SQS provides a *more accurate* depiction of the random alloy than does a single, randomly-selected 256-atom configuration. It would be interesting to compare the LDA energies of the SQS-16 with those of larger, but randomly selected supercells.<sup>17</sup>



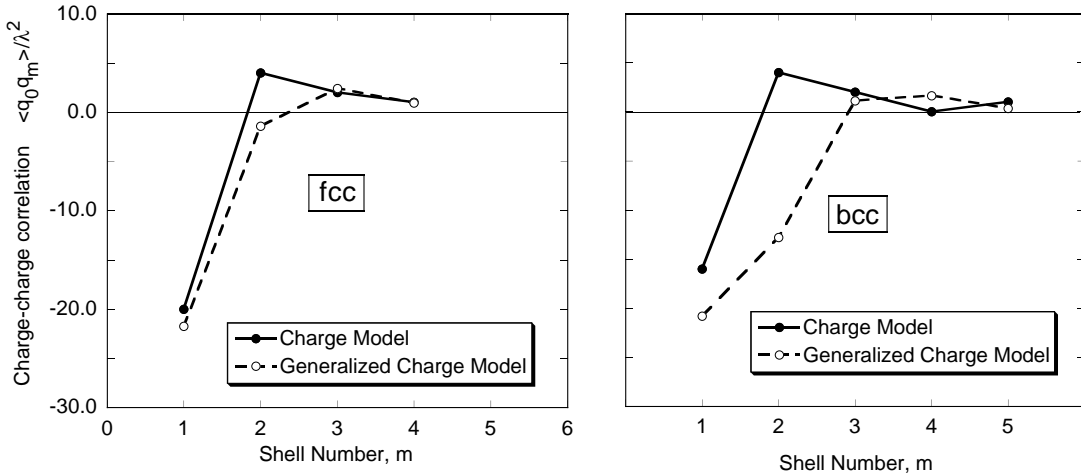


FIG. 3. Charge-charge correlation functions for random  $x=1/2$  alloys. Shown are the correlations of the simple charge model and the generalized charge model for fcc and bcc lattices. For the simple charge model, the analytic results of Eq. (23) are plotted while the correlations of the fcc (bcc) generalized charge model are obtained from a 16,384 (8,192)-atom simulation, configurationally averaged over 20 configurations. Correlation functions are shown normalized to  $\lambda_1^2$

## V. GENERALIZATIONS OF THE MODEL

### A. Summary of Successes and Failures of the Simple Model

We have thus far ascertained the physical predictions of the simple, nearest-neighbor charge model of Eq. (8), and compared them with the results of large LDA supercell calculations of Ref. 17, 18. In many cases, the simple charge model accurately predicts the electrostatic properties of LDA:

(i) The behavior of charge versus nearest neighbor environment is reproduced well by LDA calculations of fcc-based alloys (Fig. 1a).

(ii) The proportionality  $R_{\text{eff}}/R_1$  between constant-occupation-averaged charge  $\langle q \rangle_{A,B}$  and Coulomb shift  $\langle V \rangle_{A,B}$  of the model is the same as that of LDA to within a few percent (Table I).

(iii) For fcc alloys, the linear  $q - V$  relation of LDA is well reproduced (including fluctuations) by the model (Fig. 2). The model value for the slope  $\gamma/R_1$  of the  $q - V$  relation in fcc alloys is within a few percent of LDA (Table I).

(iv) The Coulomb energies of the model are extremely accurate with respect to the LDA values (to within 0.1 mRy/atom).

(v) The slope of the  $q - V$  relation,  $\gamma$ , in Fig. 2 are the same for  $A$  and  $B$ . The LDA supercell calculations also show similar slopes ( $\gamma/R_1$ ) for charges on Cu ( $-0.123$ ) or Zn ( $-0.127$ ) atoms in the fcc  $x=1/2$  alloy, or for Cu ( $-0.114$ ) or Zn ( $-0.116$ ) atoms in the bcc  $x=1/2$  alloy.

(vi) The slope of the charge *versus* number of unlike nearest neighbors (Fig. 1) are negatives of one another. LDA supercell calculations (for fcc alloys) support this (Fig. 1).

(vii) In the impurity limit, the model predicts that the charge on  $A$  embedded in pure  $B$  is equal (in magnitude)

to that of  $B$  embedded in pure  $A$ ,

$$|\langle q \rangle_A(x \rightarrow 1)| = |\langle q \rangle_B(x \rightarrow 0)| = 2Z\lambda. \quad (33)$$

The LDA supercell calculations also show this behavior (see Fig. 1), for an atom surrounded completely by unlike neighbors. Note that neither the simple model nor the LDA supercell simulations include the effects of atomic relaxations, which could likely eliminate the degeneracy of Eq. (33). [To describe relaxed configurations, it is anticipated that more parameters (e.g., bond lengths) would need to be introduced into the model.]

(viii)  $\lambda$  is composition-independent in the charge model; values of  $\lambda$  (Table I of Ref. 18) extracted from the LDA supercell calculations also demonstrate that  $\lambda$  is not sensitive to concentration. We reiterate that the charge model describes only unrelaxed configurations at a fixed volume. For lattice-mismatched systems, alloys of different composition will have different volumes, and the charge transfer will depend on this volume. To model this effect,  $\lambda$  should be explicitly volume-dependent. This *explicit* volume-dependence would lead to an *implicit* dependence of  $\lambda$  on composition. (Presumably, this implicit composition-dependence is not seen in the LDA supercell data of Ref. 18 due to the fact that the system studied, Cu-Zn, has a relatively small lattice-mismatch.) However, this should not be confused with an *explicit* composition-dependence of  $\lambda$ .

Although there are many cases of agreement between the predictions of the charge model [Eq. (8)] and the electrostatics of large LDA calculations, certain discrepancies arise in these comparisons:

(i) The LDA calculations show that the charge is not a single-valued function when plotted versus the number of unlike nearest neighbors (Fig. 1). Although there is not much width to the distribution for fcc alloys, there is a significant width for bcc alloys. Also demonstrated by Fig. 1 is that charges in the model of Eq. (8) are

quantized since the number of unlike nearest neighbors must be an integer. The LDA calculations (particularly for bcc) show no such quantization.

(ii) The slope of the  $q-V$  relation ( $\gamma/R_1$ ) for bcc alloys (Table I) is significantly larger in magnitude in the model (-0.163) than in the LDA calculations (-0.115).

(iii) There are significant fluctuations about a linear  $q-V$  relation obtained by the charge model; however, the LDA calculation show a nearly perfect linear relation with no fluctuations (Fig. 2). The fluctuations of the charge model are especially pronounced for bcc alloys.

## B. Generalizing the Model

The charge model of Eq. (8) is based on the obvious chemical fact that atomic charge results from charge *transfer*, and that the latter depends on the identity of the *neighbors*, since charge transfer does not occur between chemically equivalent sites. Thus,  $q_i$  should depend on the local environment of site  $i$ . Magri *et al.*<sup>11</sup> took first neighbors to be the “leading order” contribution to the local environment, and for the case that Magri *et al.* treated - fcc alloys - we have seen that the charge model provides an adequate description of electrostatics. However, alloys based on different lattice types can have different structural environments, in terms of coordination numbers and neighbor distances: In the fcc lattice there is a significant “gap” between the distance of the first coordination and that of the second. In bcc, however, the “gap” is after the second shell. This suggests that one generalization of the charge model which would affect bcc and fcc alloys differently is to allow the charges in the model to be dependent on more distant neighbor shells. Thus, instead of requiring the charges to be a function of the number of unlike *nearest* neighbors, we define a *generalized charge model* in which charges are a function of the number of unlike nearest neighbors *on the first several shells*  $s$  of neighbors:

$$q_i = \sum_s \lambda_s \sum_{k_s=1}^{Z_s} [\hat{S}_i - \hat{S}_{i+k_s}], \quad (34)$$

For this generalized charge model, the charge on a site  $i$  is linearly proportional to the generalized number of neighbors,  $\tilde{N}$ :

$$\tilde{N} = \sum_s N_i^{(s)} \frac{\lambda_s}{\lambda_1} \quad (35)$$

where  $N_i^{(s)}$  is the number of unlike neighbors in the  $s$ th shell for the atom at site  $i$ . In this new “generalized” charge model of Eq. (34), there are  $S$  parameters, where  $S$  is the number of shells included.

To determine the parameters of the generalized charge model, we have fit (via a least-squares procedure) the charges of the LDA supercell calculations to Eq. (34) including five shells. The parameters  $\lambda_s$  are zero, for all

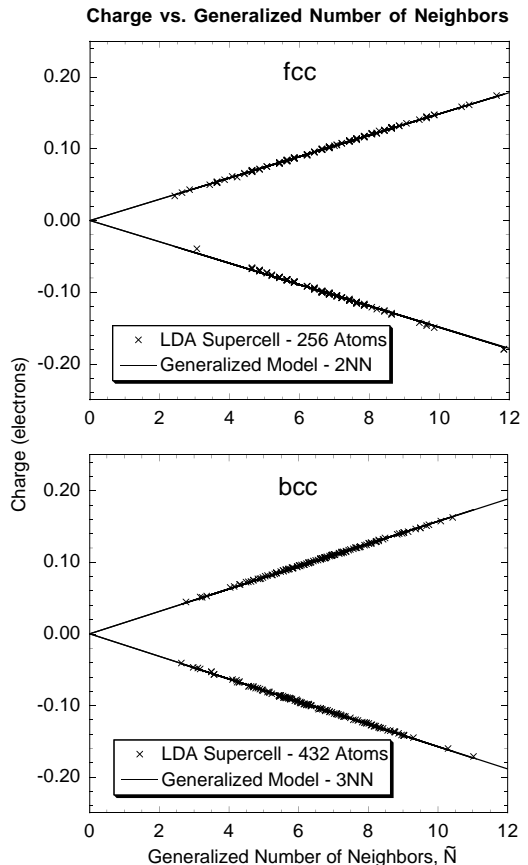


FIG. 4. Charge versus number of generalized neighbors  $\tilde{N}$  Eq. (35). Shown are the predictions of the generalized charge model of Eq. (34) using the values of  $\lambda_s$  fit to large-unit-cell LDA calculations given in Eq. (36). Also shown are the charges of the LDA large-unit-cell calculations of Ref. 18.

intents and purposes, for  $s > 2$  in fcc and  $s > 3$  in bcc. Within these ranges, we found

$$\lambda_1^{\text{fcc}} = 0.00745, \quad \lambda_2^{\text{fcc}}/\lambda_1^{\text{fcc}} = 0.214, \quad \lambda_{n>2}^{\text{fcc}}/\lambda_1^{\text{fcc}} \sim 0 \quad (36)$$

$$\lambda_1^{\text{bcc}} = 0.00786, \quad \lambda_2^{\text{bcc}}/\lambda_1^{\text{bcc}} = 0.660, \quad \lambda_3^{\text{bcc}}/\lambda_1^{\text{bcc}} = 0.0645, \quad \lambda_{n>3}^{\text{bcc}}/\lambda_1^{\text{bcc}} \sim 0. \quad (37)$$

## C. Testing the Generalized Model

We show in Figs. 3, 4, and 5 results for generalized fcc (bcc) charge models including the first two (three) neighbors shells with these values of  $\lambda_s$ .

Figure 3 shows the charge-charge correlations of random  $x=1/2$  alloys predicted by the simple charge model of Eq. (8), and the generalized charge model of Eq. (34). Although there are currently no LDA results with which to compare (due to the size of the current LDA supercells), we note that the generalized charge model changes the sign of the second neighbor correlation in both fcc and bcc relative to the simple model. It would be interesting

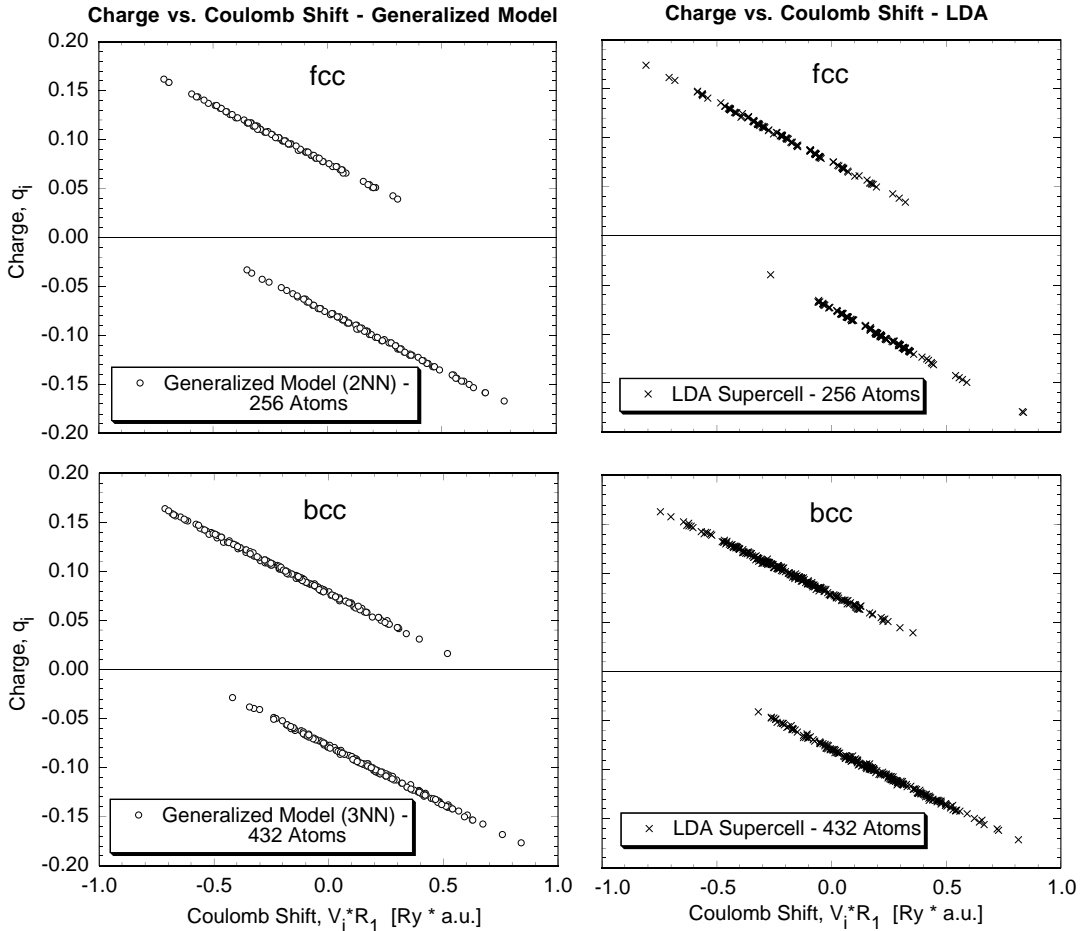


FIG. 5. Charge versus Coulomb shift as predicted by the generalized charge model of Eq. (34) using the values of  $\lambda_s$  and  $R_1$  given in Eqs. (36) and (30).

to compare these correlations with those of LDA when larger supercell calculations become available.

The charge  $q_i$  versus the generalized number of neighbors  $\tilde{N}$  is shown in Fig. 4 for LDA and for the model of Eq. (34). For fcc alloys, the corrections induced by generalizing the charge model are small since the original model of Eq. (8) is already very good. The predictions of the generalized charge model fit the LDA supercell data extremely well even for bcc alloys, where the nearest-neighbor model of Eq. (8) was lacking.

Figure 5 shows the relation between charge  $q_i$  and Coulomb shift  $V_i$  of the generalized charge model, comparing the results with LDA. Like LDA, the generalized charge model predicts a linear relation between  $q_i$  and  $V_i$  with almost no fluctuations. Furthermore, the slope of these linear relations are in excellent agreement with the LDA supercell data (Table I), provided that cutoffs for fcc and bcc are at second and third neighbor shells, respectively. Thus, the generalized charge model of Eq. (34) rectifies all of the discrepancies noted above (Section VA) between model and LDA calculations. [The fcc model for nearest-neighbors only is already accurate with respect to LDA calculations (Figs. 1 and 2), thus generalizing the fcc charge model to first- and second-neighbors

does not produce a large effect.] In Fig. 6, we show the values of the parameters  $\lambda_s$  versus distance of the shell  $s$ . One can see that the parameters are reasonably well fit by an exponential function

$$\lambda_s = \frac{\lambda_1 R_1}{R_s} e^{-(R_s - R_1)/R_0} \quad (38)$$

with a decay length of  $R_0 = 0.34R_1$ . This suggests that in an alloy the net charge on each site is screened effectively in a very short range.

Since the generalized charge model predicts a linear  $q - V$  relation in disordered alloys, with almost no fluctuations, one can also obtain a generalized model of the *Coulomb shifts* in an alloy

$$V_i \propto \gamma/R_1 \left( \sum_s \lambda_s \sum_{k_s=1}^{Z_s} [\hat{S}_i - \hat{S}_{i+k_s}] \right). \quad (39)$$

Thus, the Coulomb shifts, like the charges, depend only on the occupation of the first few neighboring shells.

#### D. Extracting Values of $\lambda$ from LDA: Supercell-Size-Dependence

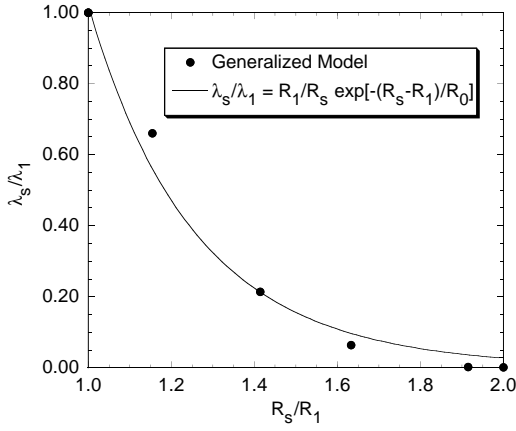


FIG. 6. Charge transfer parameters  $\lambda_s$  of generalized model of Eq. (34) as a function of distance. Also shown is a fit to the parameters to the exponential function of Eq. (38). The fitted value is  $R_0 = 0.34R_1$ .

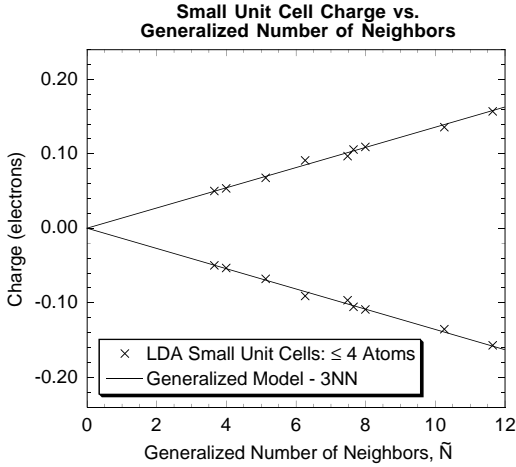


FIG. 7. Charge versus number of generalized neighbors  $\tilde{N}$  Eq. (35). Shown are the predictions of the generalized charge model of Eq. (34) using the values of  $\lambda_s$  fit to small-unit-cell data given in Eq. (40). Also shown are the charges of the LAPW small-unit-cell calculations of the present work.

We have demonstrated the validity of the generalized model of point charges and shown how the parameters of the model  $\lambda_s$  may be extracted from large-unit-cell LDA calculations. However, the models of point charges (both the simple and generalized models) assume that the *physical mechanism* underlying excess charge on a site is the same for ordered and random alloys. This suggests that the values of  $\lambda_s$  could be obtained from small-unit-cell calculations. For computational simplicity, one should know whether it is equally valid to extract values of  $\lambda_s$  from ordered or random alloys, and whether one can use LDA calculations of small cells ( $\sim 2-4$  atoms) to extract the values of  $\lambda_s$ . To this end, we have complemented the large unit-cell LDA calculations of Faulkner *et al.*<sup>17</sup> on random bcc Cu-Zn alloys by performing calculations of several *ordered small-unit-cell* bcc-based Cu-Zn ordered compounds. We use the linearized augmented plane wave

(LAPW) method.<sup>29</sup> The ordered structures considered are all bcc superlattices:  $\text{Cu}_1\text{Zn}_1$  (001),  $\text{Cu}_2\text{Zn}_2$  (111),  $\text{Cu}_2\text{Zn}_2$  (001),  $\text{Cu}_2\text{Zn}_1$  (001),  $\text{Cu}_3\text{Zn}_1$  (111), and  $\text{Cu}_1\text{Zn}_1$  (101). All of these compounds have 2-4 atoms/cell and the first five are commonly referred to by their Strukturbericht designations: *B2*, *B32*, *B11*, *C11b*, and *D0<sub>3</sub>*, respectively. In the LAPW calculations, we have used the exchange correlation of Wigner.<sup>30</sup> The muffin-tin radii are chosen to be equal (2.2 a.u.) for both Cu and Zn. Brillouin-zone integrations are performed using the equivalent  $\mathbf{k}$ -point sampling method<sup>31</sup>. Since the charge model is appropriate only for charges in unrelaxed geometries at fixed volume, all computations were done in ideal geometries at a single volume ( $a=5.56$  a.u.), even though several compositions are considered. The excess charges were extracted from the LAPW calculations by integrating the charge density inside the muffin-tin spheres and dividing the interstitial charge evenly between the atoms in the unit cell.

The LAPW charges for the six small-unit-cell compounds calculated were fit to a form of the generalized charge model of Eq. (34) with 1st-3rd neighbor shells. The parameters of the generalized model fit to these small unit-cell calculations,

$$\lambda_1^{\text{bcc}} = 0.00680, \quad \lambda_2^{\text{bcc}}/\lambda_1^{\text{bcc}} = 0.609, \quad \lambda_3^{\text{bcc}}/\lambda_1^{\text{bcc}} = 0.131, \quad (40)$$

agree well with those fit to large unit-cell data [Eq. (36)].<sup>32</sup> The parameters of Eq. (40) fit to small-unit-cell LDA calculations lead to a  $q-V$  relation which is linear, with no fluctuations, and has a slope of  $\gamma/R_1=0.112$ , compared with  $\gamma/R_1=0.119$  for the parameters of the generalized model fit to large-unit-cell LDA data. The charges extracted from small-unit-cell LDA calculations are shown in Fig. 7 as a function of generalized number of neighbors  $\tilde{N}$  [using the values of  $\lambda_s$  in Eq. (40)]. These calculations demonstrate that the parameters of the generalized model may be determined from calculations of several small-unit-cell ordered compounds in unrelaxed geometries at fixed volume. If one wishes to assess the explicit volume-dependence of the parameters, one only needs to repeat these types of calculations at a few different volumes. We have performed such volume-dependent calculations at  $a=5.36$  and  $a=5.75$  (in addition to the  $a=5.56$  calculations described above), and find that the values of  $\lambda$  only have a slight volume-dependence in this range: The value of  $\lambda_1$  at  $a=5.36$  is about 6% larger in magnitude than  $\lambda_1$  at  $a=5.75$ . Also, in this volume range the ratios  $\lambda_2/\lambda_1$  and  $\lambda_3/\lambda_1$  vary by less than their uncertainty due to the fit.

## VI. CONCLUSIONS

Recent<sup>17,18</sup> large scale (256-432 atom) local density approximation (LDA) supercell calculations of  $\text{Cu}_{1-x}\text{Zn}_x$  random alloys allow us to examine the adequacy of simple models describing the dependence of point charges in

disordered alloys on the atomic environment. We find that a model in which the excess charge  $q_i$  on an atom in an ordered or random alloy depends linearly on the number  $N_i^{(1)}$  of unlike neighbors in its first coordination shell correctly describes the trends in charge versus number of unlike nearest neighbors, (particularly for fcc alloys), the magnitudes of Coulomb energies in random  $\text{Cu}_{1-x}\text{Zn}_x$  alloys, and the relationships between *constant-occupation-averaged* charges  $\langle q_i \rangle$  and Coulomb shifts  $\langle V_i \rangle$  in the random alloy. However, for bcc alloys the *fluctuations* predicted by the model in the  $q_i$  vs  $V_i$  relation exceed those found in the LDA supercell calculations. Although we found that the fluctuations present in the model have a vanishing contribution to the electrostatic energy, generalizing the bcc (fcc) model to include a dependence of the charge on the atoms in the first *three (two) shells* (rather than the first shell only) removes the fluctuations from the model, in complete agreement with the LDA data.

Other possible generalizations of the charge model include: (i) non-linearities in the charge as a function of number of neighbors and (ii) charges which depend not only on the *number* of nearest neighbors, but also on the particular arrangement of the neighbors. This type of dependence would lead to not only pair correlations among charges, but also multibody correlations. Currently, there are no indications that these types of generalizations are warranted.

We thank Drs. Y. Wang and G. M. Stocks for providing us their LDA data of Ref.<sup>17</sup>. We also thank Dr. Z.-W. Lu for insightful discussions. This work was supported by the Office of Energy Research (OER) [Division of Materials Science of the Office of Basic Energy Sciences (BES)], U. S. Department of Energy, under contract No. DE-AC36-83CH10093.

### APPENDIX A: Analytic Derivation of the $q_i - \bar{V}_i$ Relation Within the Charge Model of Eq. (8).

Here we derive the  $q - V$  relation predicted by the charge model [Eq. (8)], averaging over any fluctuations. Consider a random  $A_{1-x}B_x$  alloy at  $x = 1/2$  with nearest neighbor coordination  $Z_1$  and an  $A$  atom at a central site, denoted by  $A(0)$ . (There is no loss of generality by choosing this atom to be  $A$ .) The charge on  $A(0)$  has the distribution  $q_M = -2M\lambda$  ( $M = 0, Z_1$ ) with the probability

$$\rho_M = \frac{1}{2^{Z_1}} \binom{Z_1}{M} \quad (41)$$

Therefore, the energy of the random alloy is

$$\langle E_M \rangle = \frac{1}{2} \sum_{M=0}^{Z_1} \rho_M q_M \sum_m \frac{1}{R_m} q_m(M) \quad (42)$$

where  $q_m(M)$  is the sum of charge on the  $m$ th shell surrounding  $A(0)$  under the constraint that there are  $M$   $B(1)$  atoms on the nearest neighbor shell.  $R_m$  is the distance of the  $m$ th shell atom from  $A(0)$ .  $\langle E_M \rangle$  can also be written as

$$\langle E_M \rangle = \frac{1}{2} \sum_{M=0}^{Z_1} \rho_M q_M \bar{V}_M \quad (43)$$

where  $\bar{V}_M$  is the Coulomb shift on the central site, averaged over all configurations where there are  $M$   $B(1)$  atoms on the nearest neighbor shell. Thus, we need to determine  $\bar{V}_M$  as a function of  $q_M = -2M\lambda$  where

$$\bar{V}_M = \sum_m \frac{1}{R_m} q_m(M). \quad (44)$$

In order to compute  $\bar{V}_M$ , we first need to compute  $q_m(M)$ .

*First Shell:* For the nearest-neighbor shell,  $m=1$ ,

$$q_1(M) = Mq_1^B + (Z_1 - M)q_1^A \quad (45)$$

For the  $Z_1$  nearest neighbors of an atom in this first shell, one is  $A(0)$ ,  $K_1$  are also nearest neighbors of  $A(0)$ , and  $\tilde{Z} = Z_1 - K_1 - 1$  are remaining. For each  $A(1)$ , the probability that it has  $n$   $B$  neighbors (i.e., with charge  $-2n\lambda$ )  $l$  of them come from atoms which are not neighbors of  $A(0)$  is

$$\rho_{n,l}^{A(1)} = \binom{\tilde{Z}}{l} \frac{1}{2^{Z_1 - K_1 - 1}} \frac{\binom{M}{K} \binom{Z_1 - 1 - M}{K_1 - K}}{\binom{Z_1 - 1}{K_1}} \quad (46)$$

where  $K = n - l$  and the following inequalities must be satisfied

$$\begin{aligned} 0 &\leq n \leq Z_1 - 1 \\ 0 &\leq l \leq n; l \leq \tilde{Z} \\ 0 &\leq n - l \leq K_1 \\ n - l &\leq M \\ K_1 - (n - 1) &\leq Z_1 - 1 - M \end{aligned} \quad (47)$$

Similarly, for each  $B(1)$ , the probability that it has  $n$   $A$  neighbors (i.e., with charge  $2n\lambda$ ),  $l$  of them which are not neighbors of  $A(0)$  is:

$$\rho_{n,l}^{B(1)} = \binom{\tilde{Z}}{l} \frac{1}{2^{Z_1 - K_1 - 1}} \frac{\binom{Z_1 - M}{K} \binom{M - 1}{K_1 - K}}{\binom{Z_1 - 1}{K_1}} \quad (48)$$

where  $K = n - l - 1$  and the following inequalities must be satisfied

$$\begin{aligned} 1 &\leq n \leq Z_1 \\ 0 &\leq l \leq n - 1; l \leq \tilde{Z} \\ 0 &\leq n - 1 - l \leq K_1 \\ n - 1 - l &\leq Z_1 - M \\ K_1 - (n - 1 - l) &\leq M - 1 \end{aligned} \quad (49)$$

Combining Eqs. (45-49), we have

$$\begin{aligned} q_1(M) &= (Z_1 - M) \sum_{n=0}^{Z_1 - 1} -2n\lambda \sum_{l=0}^n \rho_{n,l}^{A(1)} \\ &+ M \sum_{n=1}^{Z_1} 2n\lambda \sum_{l=0}^{n-1} \rho_{n,l}^{B(1)} \end{aligned} \quad (50)$$

where  $\rho_{n,l}^{A(1)}$  and  $\rho_{n,l}^{B(1)}$  are subject to the constraints (47) and (49).

*More Distant Neighbor Shells:* For  $m > 1$ ,

$$q_m(M) = \frac{Z_m}{2} [q_m^A + q_m^B] \quad (51)$$

Atoms on the  $m$ th shell have  $Z_1$  nearest neighbors,  $K_m$  of them are also nearest neighbors of  $A(0)$ . Therefore,

$$\rho_{n,l}^{A(m)} = \binom{Z_1 - K_m}{l} \frac{1}{2^{Z_1 - K_m}} \frac{\binom{M}{K} \binom{Z_1 - M}{K_m - K}}{\binom{Z_1}{K_m}} \quad (52)$$

where  $K = n - l$  and the following inequalities must be satisfied

$$\begin{aligned} 0 &\leq n \leq Z_1 \\ 0 &\leq l \leq n; l \leq Z_1 - K_m \\ 0 &\leq n - l \leq K_m \\ n - l &\leq M \\ K_m - (n - l) &\leq Z_1 - M \end{aligned} \quad (53)$$

and

$$\rho_{n,l}^{B(m)} = \binom{Z_1 - K_m}{l} \frac{1}{2^{Z_1 - K_m}} \frac{\binom{Z_1 - M}{K} \binom{M}{K_m - K}}{\binom{Z_1}{K_m}} \quad (54)$$

where  $K = n - l$ , subject to the following constraints

$$\begin{aligned} 0 &\leq n \leq Z_1 \\ 0 &\leq l \leq n; l \leq Z_1 - K_m \\ 0 &\leq n - l \leq K_m \\ n - l &\leq Z_1 - M \\ K_m - (n - l) &\leq M \end{aligned} \quad (55)$$

Combining Eqs. (51-55), we have

$$q_m(M) = \frac{1}{2} Z_m \sum_{n=0}^{Z_1} 2n\lambda \sum_{l=0}^n [\rho_{n,l}^{B(m)} - \rho_{n,l}^{A(m)}] \quad (56)$$

where  $\rho_{n,l}^{A(m)}$  and  $\rho_{n,l}^{B(m)}$  are subject to the constraints (53) and (55). Note that  $q_m(M) = 0$  for any shell which does not share nearest neighbors with  $A(0)$  (i.e.,  $K_m = 0$ ). Using the above derived values of  $q_1(M)$  and  $q_m(M)$  in Eq. (44), we may determine  $\bar{V}_M$  as a function of  $q_M = -2M\lambda$ , and as a function of  $M$  this relation is precisely linear, with no fluctuations:

$$q_M \propto \bar{V}_M. \quad (57)$$

## APPENDIX B: Structural Information for SQS-16

The ideal (unrelaxed) fcc-based SQS-16 structure ( $A_8B_8$ ) has orthorhombic symmetry and primitive lattice vectors

$$\mathbf{a} = \left(\frac{1}{2}, \frac{1}{2}, 0\right)a; \quad \mathbf{b} = (1, -1, 2)a; \quad \mathbf{c} = (1, -1, -2)a \quad (58)$$

The 16 atomic positions, in Cartesian coordinates, are

$$\begin{aligned} A &: (0, 0, 0)a \\ B &: \left(\frac{1}{2}, 0, \frac{1}{2}\right)a \\ A &: \left(\frac{1}{2}, -\frac{1}{2}, 1\right)a \\ B &: \left(1, -\frac{1}{2}, \frac{3}{2}\right)a \\ A &: \left(1, -\frac{1}{2}, -\frac{3}{2}\right)a \\ A &: (1, -1, -1)a \\ B &: \left(\frac{3}{2}, -1, -\frac{1}{2}\right)a \\ A &: \left(\frac{3}{2}, -\frac{3}{2}, 0\right)a \\ B &: \left(\frac{1}{2}, -\frac{1}{2}, -1\right)a \\ A &: \left(1, -\frac{1}{2}, -\frac{1}{2}\right)a \\ B &: (1, -1, 0)a \\ A &: \left(\frac{3}{2}, -1, \frac{1}{2}\right)a \\ A &: \left(\frac{1}{2}, 0, -\frac{1}{2}\right)a \\ B &: \left(\frac{1}{2}, -\frac{1}{2}, 0\right)a \\ B &: \left(1, -\frac{1}{2}, \frac{1}{2}\right)a \\ B &: (1, -1, 1)a. \end{aligned} \quad (59)$$

The SQS-16 structure matches the first seven pair correlation functions of the random  $x = 1/2$  alloy exactly.

<sup>1</sup> A recent review is given in A. Zunger, in *Statics and Dynamics of Alloy Phase Transformations*, edited by P. E. A. Turchi and A. Gonis, NATO ASI Series (Plenum, New York, 1994) p. 361.

<sup>2</sup> S. -H. Wei, L. G. Ferreira, and A. Zunger, Phys. Rev. B **41**, 8240 (1990); L. G. Ferreira, S. -H. Wei, and A. Zunger, Phys. Rev. B **40**, 3197 (1989); S. -H. Wei, A. A. Mbaye, L. G. Ferreira, and A. Zunger, Phys. Rev. B **36**, 4163 (1987)

<sup>3</sup> M. Sluiter, D. de Fontaine, X. Q. Guo, R. Poloucky, and A. J. Freeman, Phys. Rev. B **42**, 10460 (1990).

- <sup>4</sup> J. M. Sanchez, J. P. Stark, and V. L. Moruzzi, Phys. Rev. B **44**, 5411 (1991).
- <sup>5</sup> Z. -W. Lu, S. -H. Wei, A. Zunger, S. Frota-Pessoa, and L. G. Ferreira, Phys. Rev. B **44**, 512 (1991);
- <sup>6</sup> M. Asta, D. de Fontaine, and M. van Schilfgaarde, J. of Mat. Res. **8**, 2554 (1993).
- <sup>7</sup> Z. -W. Lu and A. Zunger, Phys. Rev. B **50**, 6626 (1994); Z. -W. Lu, D. B. Laks, S. -H. Wei, and A. Zunger, Phys. Rev. B **50**, 6642 (1994).
- <sup>8</sup> C. Wolverton and A. Zunger, Phys. Rev. B **52**, 8813 (1995).
- <sup>9</sup> A. Zunger, S.-H. Wei, L. G. Ferreira, and J. E. Bernard, Phys. Rev. Lett. **65**, 352 (1990); S.-H. Wei, L. G. Ferreira, J. E. Bernard, and A. Zunger, Phys. Rev. B **42**, 9622 (1990); S.-H. Wei and A. Zunger, Phys. Rev. B **43**, 1662 (1991).
- <sup>10</sup> Z. W. Lu, S. -H. Wei, and A. Zunger, Phys. Rev. B **44**, 3387 (1991); **44**, 10470 (1991); **45**, 10314 (1992).
- <sup>11</sup> R. Magri, S. -H. Wei, and A. Zunger, Phys. Rev. B **42**, 11388 (1990).
- <sup>12</sup> A. Borici and R. Monnier, Phys. Rev. B **47**, 6768 (1993).
- <sup>13</sup> D. D. Johnson and F. J. Pinski, Phys. Rev. B **48**, 11553 (1993).
- <sup>14</sup> C. Wolverton and A. Zunger, Phys. Rev. B **51**, 6876 (1995).
- <sup>15</sup> A. V. Ruban, I. A. Abrikosov, and H. L. Skriver, Phys. Rev. B **51**, 12958 (1995).
- <sup>16</sup> Y. Wang, G. M. Stocks, W. A. Shelton, D. M. C. Nicholson, Z. Szotek, and W. M. Temmerman, Phys. Rev. Lett. **75**, 2867 (1995).
- <sup>17</sup> J. S. Faulkner, Y. Wang, and G. M. Stocks Phys. Rev. B **52**, 17106 (1995).
- <sup>18</sup> J. S. Faulkner, Y. Wang, and G. M. Stocks, in *Alloy Modeling and Design*, G. M. Stocks, C. T. Liu, and P. E. A. Turchi, eds. (The Minerals, Metals, and Materials Society, Warrendale, PA) 1995; J. S. Faulkner, Y. Wang, and G. M. Stocks, in *Stability of Materials*, NATO ASI Series E: Applied Sciences, A. Gonis, P. E. A. Turchi, and J. Kudrnovsky, eds. (Kluwer, Boston) 1996.
- <sup>19</sup> For a review of the coherent potential approximation, see B. L. Gyorffy, D. D. Johnson, F. J. Pinski, D. M. Nicholson, and G. M. Stocks, in *Alloy Phase Stability*, edited by G. M. Stocks and A. Gonis (Kluwer, Dordrecht, 1989), p. 293; F. Ducastelle, *Order and Phase Stability in Alloys* (North-Holland, New York, 1991); G. M. Stocks *et al.*, in *Statics and Dynamics of Alloy Phase Transformations*, P. E. A. Turchi and A. Gonis, eds., NATO ASI Series, (Plenum, New York, 1994).
- <sup>20</sup> D. D. Johnson, D. M. Nicholson, F. J. Pinski, B. L. Gyorffy, and G. M. Stocks, Phys. Rev. B **41**, 9701 (1990).
- <sup>21</sup> F. J. Pinski, B. Ginatempo, D. D. Johnson, J. B. Staunton, G. M. Stocks, and B. L. Gyorffy, Phys. Rev. Lett. **66**, 766 (1991).
- <sup>22</sup> P. E. A. Turchi, M. Sluiter, F. J. Pinski, D. D. Johnson, D. M. Nicholson, G. M. Stocks, and J. B. Staunton, Phys. Rev. Lett. **67** 1779 (1991).
- <sup>23</sup> J. B. Staunton, D. D. Johnson, and F. J. Pinski Phys. Rev. B **50**, 1450 (1994). D. D. Johnson, J. B. Staunton, and F. J. Pinski Phys. Rev. B **50**, 1473 (1994).
- <sup>24</sup> P. Weinberger, V. Drchal, L. Szunyogh, J. Fritscher, and B. I. Bennett, Phys. Rev. B **49**, 13366 (1994).
- <sup>25</sup> I. A. Abrikosov, Yu. H. Vekilov, P. A. Korzhavyi, A. V. Ruban, and L. E. Skilkrot, Solid State Commun. **83**, 867 (1992).
- <sup>26</sup> P. A. Korzhavyi, A. V. Ruban, S. I. Simak, and Yu. Kh. Vekilov, Phys. Rev. B **49**, 14229 (1994); P. A. Korzhavyi, A. V. Ruban, I. A. Abrikosov, and H. L. Skriver, Phys. Rev. B **51**, 5773 (1995).
- <sup>27</sup> J. M. Sanchez, F. Ducastelle, and D. Gratias, Physica A **128**, 334 (1984)
- <sup>28</sup> One might imagine that the equivalence of charges in the dilute limit [Eq. (33)] could be broken by allowing different values of  $\lambda$  for  $A$  and  $B$  atoms,  $\lambda_A$  and  $\lambda_B$ . However, global neutrality would then require  $\lambda_A = \lambda_B$ .
- <sup>29</sup> S.-H. Wei and H. Krakauer, Phys. Rev. Lett. **55**, 1200 (1985); D. J. Singh, *Planewaves, Pseudopotentials, and the LAPW Method*, (Kluwer, Boston, 1994).
- <sup>30</sup> E. Wigner, Phys. Rev. **46**, 1002 (1934).
- <sup>31</sup> S. Froyen, Phys. Rev. B **39**, 3168 (1989)
- <sup>32</sup> The fact that  $\lambda_1$  fit to small-unit-cell data is about 15% smaller than that fit to large-unit-cell data is merely an artifact of the LAPW charges being about 15% smaller than the multiple scattering charges.